

2003

Orthogonal Frequency Division Multiplexing modulation and inter-carrier interference cancellation

Yao Xiao

Louisiana State University and Agricultural and Mechanical College

Follow this and additional works at: https://digitalcommons.lsu.edu/gradschool_theses



Part of the [Electrical and Computer Engineering Commons](#)

Recommended Citation

Xiao, Yao, "Orthogonal Frequency Division Multiplexing modulation and inter-carrier interference cancellation" (2003). *LSU Master's Theses*. 1619.

https://digitalcommons.lsu.edu/gradschool_theses/1619

This Thesis is brought to you for free and open access by the Graduate School at LSU Digital Commons. It has been accepted for inclusion in LSU Master's Theses by an authorized graduate school editor of LSU Digital Commons. For more information, please contact gradetd@lsu.edu.

ORTHOGONAL FREQUENCY DIVISION MULTIPLEXING MODULATION AND INTER-CARRIER INTERFERENCE CANCELLATION

A Thesis
Submitted to the Graduate Faculty of the
Louisiana State University and
Agricultural and Mechanical College
in partial fulfillment of the
requirements for the degree of
Master of Science in Electrical Engineering
In
The Department of Electrical and Computer Engineering

by
Yao Xiao
B.S., Dalian University of Technology, 1998
M.S., Institute of Automation, C.A.S, 2001
May 2003

Acknowledgments

The author wishes to thank Dr. Wu for his invaluable guidance, kindness and understanding during this research.

Table of Contents

Acknowledgments	ii
Abstract.....	v
Chapter 1 Introduction and Motivation.....	1
1.1 Introduction.....	1
1.2 Motivation.....	3
1.3 Applications	5
Chapter 2 OFDM and PAPR Problem	6
2.1. Principal OFDM Model	6
A. Overview	6
B. OFDM Modulation.....	7
C. Orthogonal Subcarriers.....	8
D. Bandpass Signaling	9
E. OFDM Demodulation.....	9
2.2 Modern OFDM model	10
A. Overview	10
B. IDFT and Orthogonality.....	11
C. Guard Interval and Cyclic Prefix.....	11
D. A Practical OFDM System- HiperLAN/2.....	13
2.3 PAPR Problem.....	14
Chapter 3 Wireless Channel	18
3.1 AWGN and Fading Channel.....	18
3.2 Rayleigh Channel.....	19
3.3 Simple Local Model.....	20
3.4 COST 207 Fading Model.....	21
3.5 Multipath Fading with CFO.....	24
Chapter 4 Intercarrier Interference Problem and Solutions	30
4.1 Factors Inducing ICI	30
A. Doppler Effect:.....	31
B. Synchronization Error	32
C. Multipath Fading	33
4.2 Intercarrier Interference and Signal-to-interference Ratio.....	34
A. ICI in Simple Local Model	34
B. ICI in Multipath Model	35
C. Signal to Interference Ratio	35
4.3 Solutions for ICI	36
A. CFO Estimation.....	36

B. Windowing	37
Chapter 5 Clustering Detection and Multiple Codebook	40
5.1 Clustering Inter-carrier Interference Cancellation	40
A. Justification of Slowly Time-varying	40
B. Clustering Method	41
C. Pilot Bits	42
D. Simulation Results	42
5.2 Multiple-Codebook	44
A. General Structure of ICI Self-cancellation.....	44
B. Comparison of Codebooks	46
5.3 Summary and Further Work	48
References	49
Vita	53

Abstract

The Orthogonal Frequency Division Multiplexing (OFDM) technique, wireless channel models, and a pair of new intercarrier interference self-cancellation methods are investigated in this thesis. The first chapter addresses the history of OFDM, along with its principles and applications. Chapter two consists of three parts: the principal, the modern OFDM models, and the Peak to Average Power Ratio (PAPR) problem. Chapter two also summarizes possible PAPR solutions. Chapter three discusses a series of well-known wireless channel models, as well as the general formula for wireless channels. In Chapter four, ICI problem has been discussed, along with its existing solutions. Chapter five focuses on two new ICI self-cancellation schemes, namely the clustering method and the multi-codebook method. These two new methods show promising results through the simulations. A summary of this thesis and the discussion of future research are also provided in Chapter five.

Chapter 1 Introduction and Motivation

This chapter consists of three parts: the introduction of OFDM history, the research motivation, and the applications of OFDM technique.

1.1 Introduction

Orthogonal frequency division multiplexing (OFDM) is one of the multi-carrier modulation (MCM) techniques that transmit signals through multiple carriers. These carriers (subcarriers) have different frequencies and they are orthogonal to each other. Orthogonal frequency division multiplexing techniques have been applied in both wired and wireless communications, such as the asymmetric digital subscriber line (ADSL) and the IEEE 802.11 standard.

It is well known that Chang proposed the original OFDM principles in 1966 [1], and successfully achieved a patent in January of 1970. Later on, Saltzberg analyzed the OFDM performance and observed that the crosstalk was the severe problem in this system. Although each subcarrier in the principal OFDM systems overlapped with the neighborhood subcarriers, the orthogonality can still be preserved through the staggered QAM (SQAM) technique. However, the difficulty will emerge when a large number of subcarriers are required. In some early OFDM applications, the number of subcarriers can be chosen up to 34. Such 34 symbols will be appended with redundancy of a guard time interval to eliminate intersymbol interference (ISI) [2].

However, should more subcarriers be required, the modulation, synchronization, and coherent demodulation would induce a very complicated OFDM requiring additional hardware cost. In 1971, Weinstein and Ebert proposed a modified OFDM system [3] in

which the discrete Fourier Transform (DFT) was applied to generate the orthogonal subcarriers waveforms. Their scheme reduced the implementation complexity significantly, by making use of the IDFT modules and the digital-to-analog converters. In their proposed model, baseband signals were modulated by the inverse DFT (IDFT) in the transmitter and then demodulated by DFT in the receiver. Therefore, all the subcarriers were overlapped with others in the frequency domain, while the DFT modulation still assures their orthogonality, as shown in Fig. 1.1.

Moreover, the windowing technique was introduced in this paper to attack the inter-symbol interference (ISI) and inter-carrier interference (ICI) problems. Thanks to these evolutions, modern low-cost OFDM systems have become plausible.

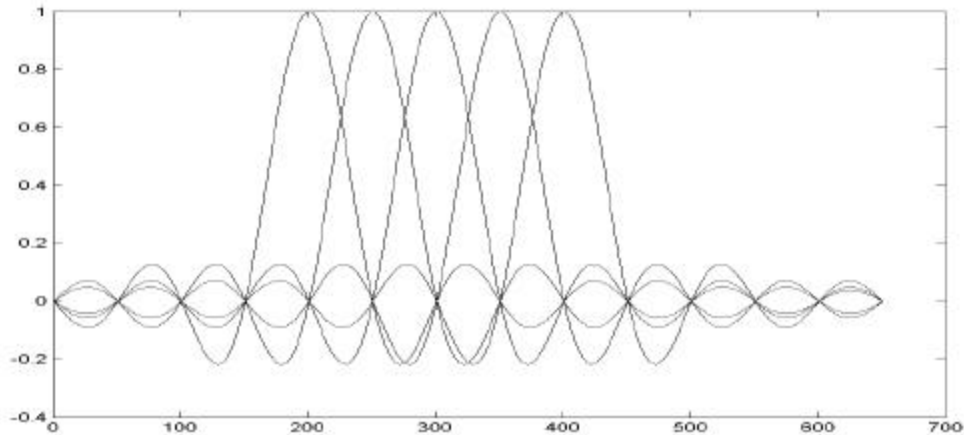


Fig. 1.1 Frequency spectrum of OFDM subcarrier signals

Cyclic prefix (CP) or cyclic extension was first introduced by Peled and Ruiz in 1980 [4] for OFDM systems. In their scheme, conventional null guard interval is substituted by cyclic extension for fully-loaded OFDM modulation. As a result, the orthogonality among the subcarriers was guaranteed. With the trade-off of the transmitting energy

efficiency, this new scheme can result in a phenomenal ICI reduction. Hence it has been adopted by the current IEEE standards.

In 1980, Hirosaki introduced an equalization algorithm to suppress both ISI and ICI [5], which may have resulted from a channel distortion, synchronization error, or phase error. In the meantime, Hirosaki also applied QAM modulation, pilot tone, and trellis coding techniques in his high-speed OFDM system, which operated in voice-band spectrum.

In 1985, Cimini introduced a pilot-based method to reduce the interference emanating from the multipath and co-channels [6]. In 1989, Kalet suggested a subcarrier-selective allocating scheme [7]. He allocated more data through transmission of “good” subcarriers near the center of the transmission frequency band; these subcarriers will suffer less channel distortion.

In the 1990s, OFDM systems have been exploited for high data rate communications. In the IEEE 802.11 standard, the carrier frequency can go up as high as 2.4 GHz or 5 GHz. Researchers tend to pursue OFDM operating at even much higher frequencies nowadays. For example, the IEEE 802.16 standard proposes yet higher carrier frequencies ranging from 10 GHz to 60 GHz.

1.2 Motivation

The demand for future higher data rate communications always provides the impetus for this research. It is obvious that a parallel system is capable of carrying more information than a cascade system, simply because it uses a variety of frequency bands. However, the significant advantage of OFDM is that it is robust in frequency-selective channels, which result from either multipath fadings or other communication

interferences. The interference problem is severe especially for some systems working in the Unlicensed National Information Infrastructure (U-NII) operating frequency range, such as the IEEE 802.11a standard. Under any of these conditions, the channel has non-uniform power gains, as well as nonlinear phases across frequencies. An example is provided in Fig. 1.2.

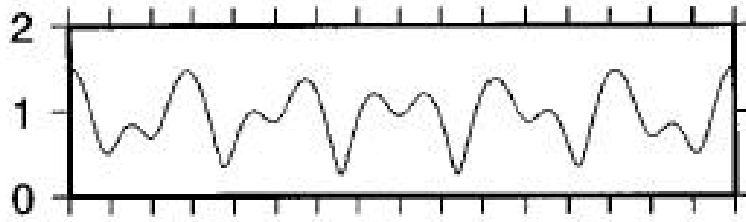


Fig. 1.2 Magnitude response of a fading channel

In order to deal with frequency-selective fadings, the transmitted OFDM signals are divided into many sub-channels so that those sub-channels can be considered frequency-flat approximately as the number of the sub-channel N is large enough. Hence the OFDM signals will suffer channel distortion less than the conventional modulated signals.

Under OFDM modulation, the symbol duration becomes N times longer. For example, if the input data rate is 20Mbps, then, the symbol duration is 50 ns; however, in an OFDM system with 128 subcarriers, the symbol duration could become 6.4 μ s. If these two kinds of symbols are modulated and transmitted through a channel with a particular *rms* value--say, *rms* = 60 ns, it is clear that the system with a longer symbol duration would perform better. In practice, the DVB-T standard suggests to use 2,048 subcarriers, or 8,192 subcarriers [8]. In these cases, the symbol duration can be even increased by several thousand times.

1.3 Applications

The OFDM techniques had been applied for ANDEFT and KINEPLEX [9], since 1960s. After the IFFT/FFT technique was introduced, the implementation of OFDM became more convenient. Generally speaking, the OFDM applications may be divided into two categories-wired and wireless technologies. In wired systems such as Asymmetric Digital Subscriber Line (ADSL) and high speed DSL, OFDM modulation may also be referred as Discrete Multitone Modulation (DMT). In addition, wireless OFDM applications may be shown in numerous standards such as IEEE 802.11 [10] and HiperLAN [11].

OFDM was also applied for the development of Digital Video Broadcasting (DVB) in Europe, which was widely used in Europe and Australia. In the DVB standards, the number of subcarriers can be more than 8,000, and the data rate could go up as high as 15Mbps [12]. At present, many people still work to modify the IEEE 802.16 standard, which may result in an even higher data rate up to 100Mbps.

Chapter 2 OFDM and PAPR Problem

In this chapter, principal and modern OFDM systems will be discussed. The principal model, as well as mathematical formulae, will be addressed to demonstrate the advantages of the OFDM technique. In addition, special problems will be explored, which might occur in OFDM systems. Finally an overview of the Peak-to-average-power Ratio (PAPR) problem will be provided in this chapter.

2.1. Principal OFDM Model

A. Overview

Since the original OFDM model was proposed in the 1960s [1], the core structure of OFDM has hardly changed. The key idea of OFDM is that a single user would make use of all orthogonal subcarrier in divided frequency bands. Therefore, the data rate can be increased significantly. Since the bandwidth is divided into several narrower subchannels, each subchannel requires a longer symbol period. Therefore OFDM systems can overcome the intersymbol interference (ISI) problem. As a consequence, the OFDM system can result in lower bit error rates but higher data rates than conventional communication systems.

Nevertheless, OFDM technique has certain drawbacks [13], such as the increased system complexity, which is associated with the generation of orthogonal subcarriers, and other new problems, which might not occur in other modulation schemes. Such new problems include the peak to average power ratio (PAPR) and inter-carrier interference (ICI). The PAPR problem will be discussed in Chapter 2, and the ICI problem will be further discussed in Chapter 4 and Chapter 5.

B. OFDM Modulation

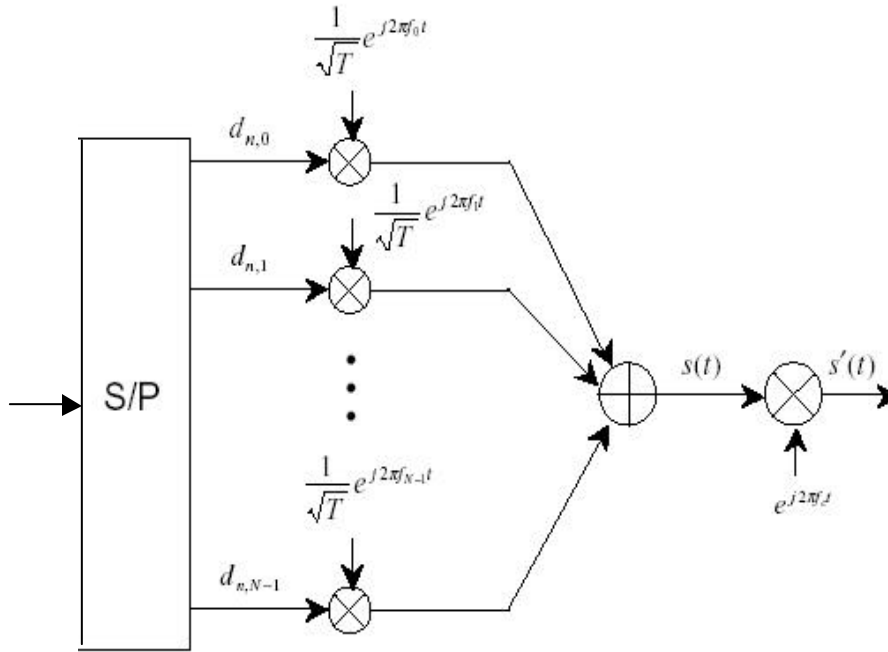


Fig 2.1 Principal OFDM modulation block diagram

As depicted in Fig 2.1, the input data stream is converted into N parallel data streams through a serial-to-parallel port. The duration of the data is elongated by N times. Serial-to-parallel conversion is depicted in Fig 2.2.

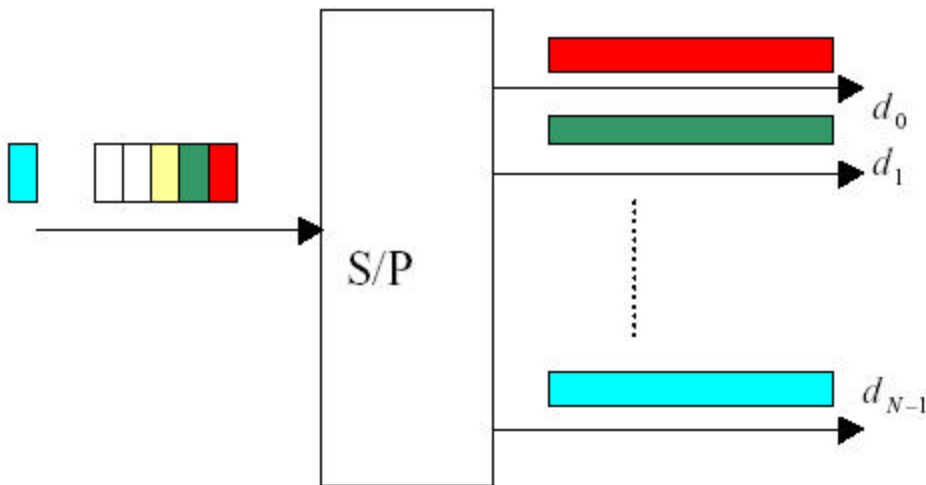


Fig 2.2 Serial to Parallel conversion

C. Orthogonal Subcarriers

When the parallel symbol streams are generated, each stream would be modulated and carried at different center frequencies as the traditional FDM scheme. The subcarriers centered at frequencies $f_0, f_1, f_2, \dots, f_{N-1}$ in Fig.2.1 must be orthogonal to each other.

The definition of the orthogonality was given in [14] as

$$\int_0^T \cos(2\pi f_n t) \times \cos(2\pi f_m t) dt = \mathbf{d}(n - m), \quad (2.1.1)$$

where $\mathbf{d}(n-m)$ is the Dirac-Delta function.

In OFDM modulation, the subcarrier frequency f_n is defined as

$$f_n = n\Delta f, \quad (2.1.2)$$

$$\text{where } \Delta f = \frac{f_s}{N} = \frac{1}{NT} \quad (2.1.3)$$

Here $f_s = \frac{1}{T}$ is the entire bandwidth, and N is the number of subcarriers.

Substituting Eq. 2.1.2 and Eq.2.1.3 into Eq.2.1.1, Orthogonality can easily be justified for all $f_0, f_1, f_2, \dots, f_{N-1}$. Fig 2.3 illustrates an example of subcarrier waveforms.

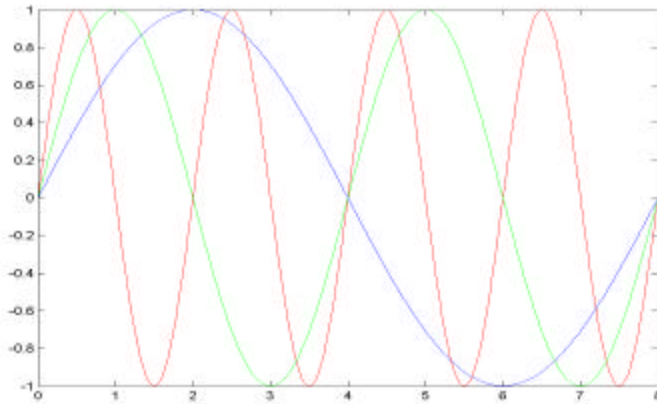


Fig 2.3 An illustration of subcarrier waveforms

D. Bandpass Signaling

After the modulation by orthogonal sub carriers, all N subcarrier waveforms were added together to be up-converted to the pass-band. This resulting signal waveform will be transmitted with a carrier frequency at 2.4G Hz, 5G Hz, 11G Hz or 60 G Hz. Then the band-pass OFDM signal waveform would be sent to power amplifier and antennas.

Thus, the transmitted OFDM signal $x(t)$ can be expressed as:

$$x(t) = \sum_{n=0}^{N-1} \frac{\exp(j2\pi(f_c + n\Delta f)t)}{\sqrt{T}} s(n), \quad (2.1.1)$$

where the $s(n)$ represents the input data stream, T the symbol duration and f_c the carrier frequency. Traveling through a wireless channel, the distorted $x(t)$ results in $r'(t)$, as shown in Fig.2.4.

E. OFDM Demodulation

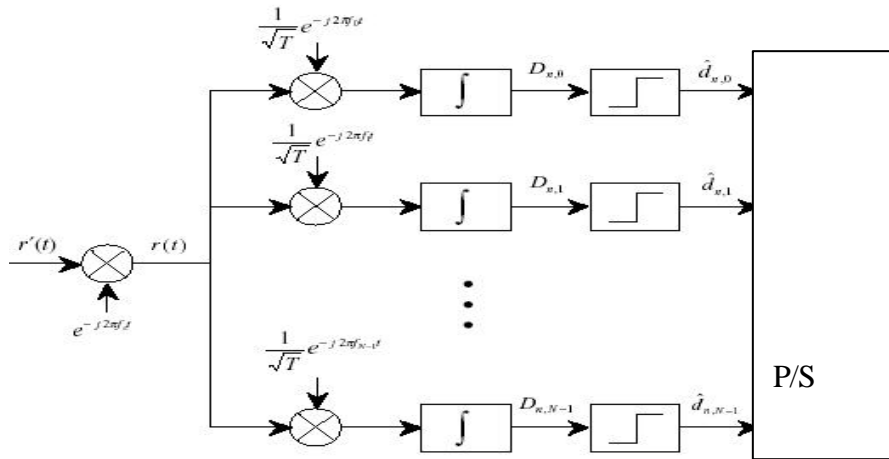


Fig 2.4 OFDM receiver

At the receiver, the received signal is down-converted to form a base-band signal first. Then, low-pass filters and de-subcarriers are applied to separate subcarrier waveforms. Orthogonality of sub-carriers will ensure that only the targeted subcarrier

waveform will be preserved in each sub-band. Ideally, the final detected symbols will be identical to those transmitted in Fig.2.1.

2.2 Modern OFDM model

A. Overview

It was a complicated process to achieve N subcarrier oscillators, especially when the N was large. Therefore, the principal OFDM model could not be widely used. Thanks to IDFT/DFT-based algorithms introduced in 1980 [3], OFDM has become a popular wireless modulation technique since after. The modern OFDM model is depicted in Fig 2.5.

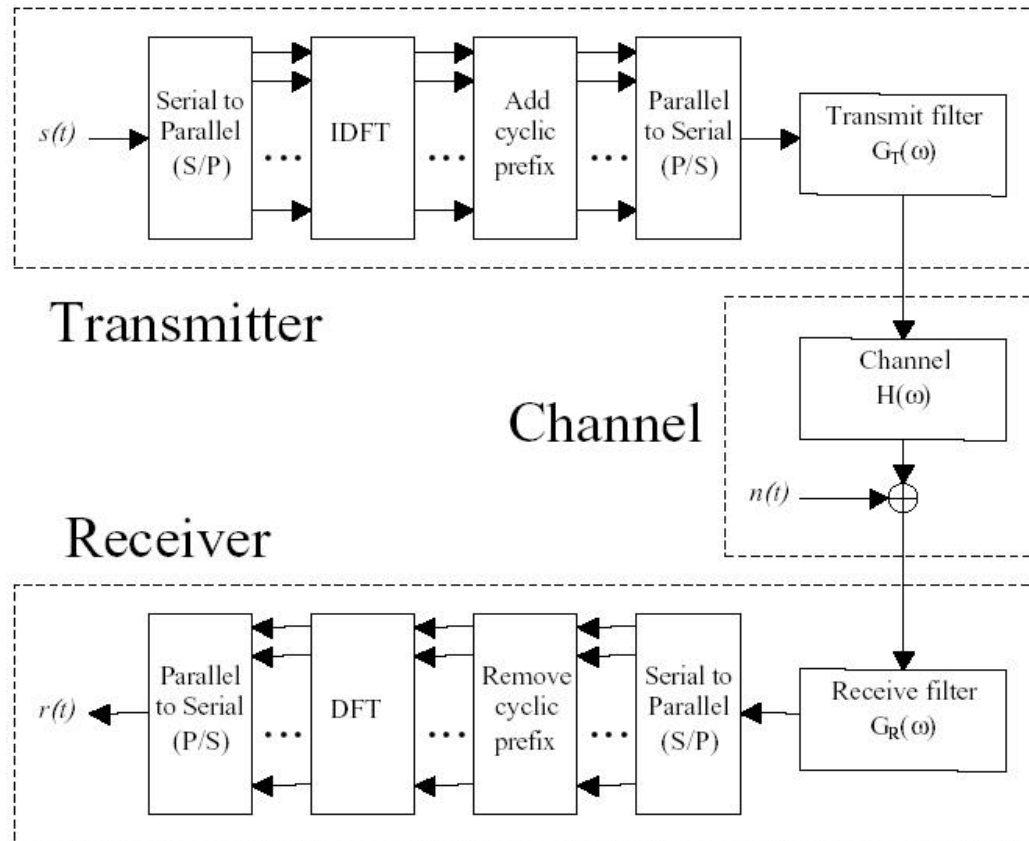


Fig 2.5 Modern OFDM system

B. IDFT and Orthogonality

After the parallel symbol streams are generated, IDFT operator substitutes the aforementioned local subcarrier oscillators. IDFT operation, $F(n) \xrightarrow{IDFT} f(k)$, can be written as [15]:

$$f(k) = \frac{1}{\sqrt{N}} \sum_{n=0}^{N-1} F(n) \exp\left(\frac{j2\pi kn}{N}\right) \quad (2.2.1)$$

The orthogonality of discrete-time Fourier bases can be described as follows:

$$\sum_{k=0}^{N-1} \cos\left(\frac{2\pi kn}{N}\right) \times \cos\left(\frac{2\pi km}{N}\right) = \mathbf{d}(n - m) \quad (2.2.2)$$

Clearly, the output sequences of the IDFT are orthogonal to each other. With the absence of local oscillators, the OFDM system complexity has been greatly reduced.

C. Guard Interval and Cyclic Prefix

In Fig 2.5, the block denoted as “Add Cyclic Prefix” actually should be called the “Add Guard Interval” in general. The cyclic prefix (CP) is the most common guard interval (GI). The GI is introduced initially to eliminate the inter block interference (IBI). Since one block of input data symbols are associated with a single transmitted waveform in an OFDM system, most people refer IBI as ISI. Fig 2.6 demonstrates how to use the GI to eliminate the ISI.

However, multipath fading channel models are concerned in most situations. Therefore, many time-delayed versions of the transmitted waveform might be found at the receiver [16]. Without GI, these waveforms would interfere with each other, just as demonstrated in the top half of Fig.2.6. Nevertheless, in those cases where the GI was employed, the portions of waveforms received in the GI duration would be totally discarded, as shown in the bottom half of Fig.2.6. Thus, the ISI could be completely

eliminated accordingly. It is noted that the GI duration must be larger than the maximum channel delay time. Otherwise, it could not entirely remove the ISI.

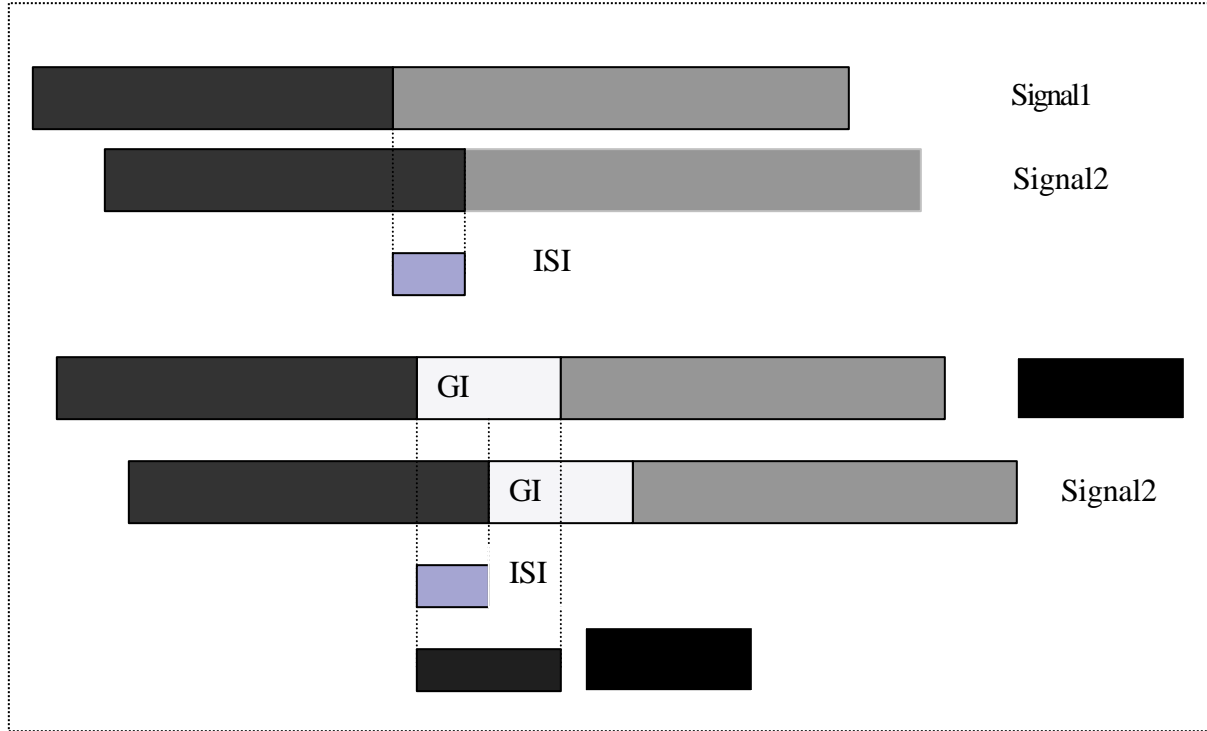


Fig.2.6 Guard Interval Elimination of the ISI

There are several options for GI. One choice of GI is zero padding. In this scheme, no waveform is transmitted in the GI duration. However, the zero-padded waveform would destroy the orthogonality of subcarriers and results in intercarrier interference (ICI).

The cyclic prefix (CP) is a good substitute of the zero-padding GI. In the CP scheme, the GI is a copy of the partial waveform. Based on the fact that the Fourier bases are periodic functions, the orthogonality of subcarriers can be preserved consequently.

As depicted in Fig 2.7, an end-portion of waveform is copied and inserted prior to the beginning of waveform. The time duration of CP, denoted as T_G in the Fig 2.7, is often chosen according to the following:

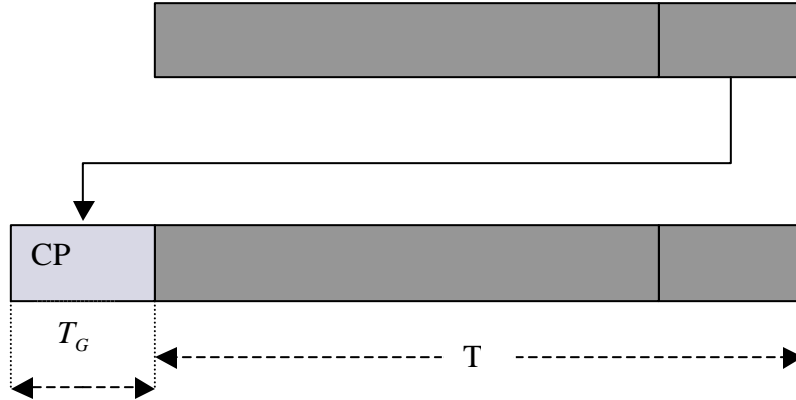


Fig 2.7 Generate Cyclic Prefix

Let k be an integer in Eq. 2.2.3

$$T_G = \frac{T}{2^k}. \quad (2.2.3)$$

For example, in the IEEE 802.11a standard, $k = 2$ is chosen; in Europe DVB (Digital Video Broadcasting) standards, $k = 1, 2, \dots, 6$ can be employed. As aforementioned, k should also depend on the maximum delay time of the channel. When CP is applied instead of zero-padding GI, both ICI and ISI are eliminated.

D. A Practical OFDM System- HiperLAN/2

Even though there are many applications of the OFDM technique, the corresponding parameters vary from one to another and depend on the practical purposes. Fig 2.8 illustrates the simplified version of a practical OFDM system--the HiperLAN/2 system. As a wireless LAN model, the HiperLAN/2 standard can provide services at 54 Mbps data-rate. The European Telecommunication Standards Institute (ETSI) and Broadband Radio Access Network (BRAN) originally proposed this standard. At present, it has been widely applied in airports, homes, and universities in Europe, Australia and Japan. In this standard, many techniques such as QAM, convolution

coding, puncture, and interleaver might be used. At the receiver, there are de-interleaver, zero-inserting, and Viterbi decoder components correspondingly.

The OFDM modulation in the HiperLAN/2 system is similar the principal one, except that four pilot bits were used for the time and frequency synchronization, and CP is inserted prior to the OFDM information symbols, as depicted in Fig 2.5 and 2.7. As a matter of fact, the HiperLAN/2 standard is nearly the same as the IEEE 802.11a standard at the physical layer; both standards use 64 subcarriers with 16 cyclic prefix bits per block.

2.3 PAPR Problem

One of the new problems emerging in OFDM systems is the so-called Peak to Average Power Ratio (PAPR) problem. The input symbol stream of the IFFT should possess a uniform power spectrum, but the output of the IFFT may result in a non-uniform or spiky power spectrum. Most of transmission energy would be allocated for a few instead of the majority subcarriers. This problem can be quantified as the PAPR measure.

PAPR is defined as the peak signal power versus the average signal power.

$$PAPR = \frac{\text{Max}\{|X_i|^2\}}{E\{|X_i|^2\}},$$

where X_i is the i^{th} bit in an IFFT output stream

This high PAPR is undesirable, because it generally would result in out-of-band (OOB) distortion power.

The PAPR problem can be illustrated in Fig 2.9. In this example, the average power is 1, and peak power is about 5.

HiperLAN/2 - 16QAM mode with 3/4 code rate (4/6 P2 puncturing rate).

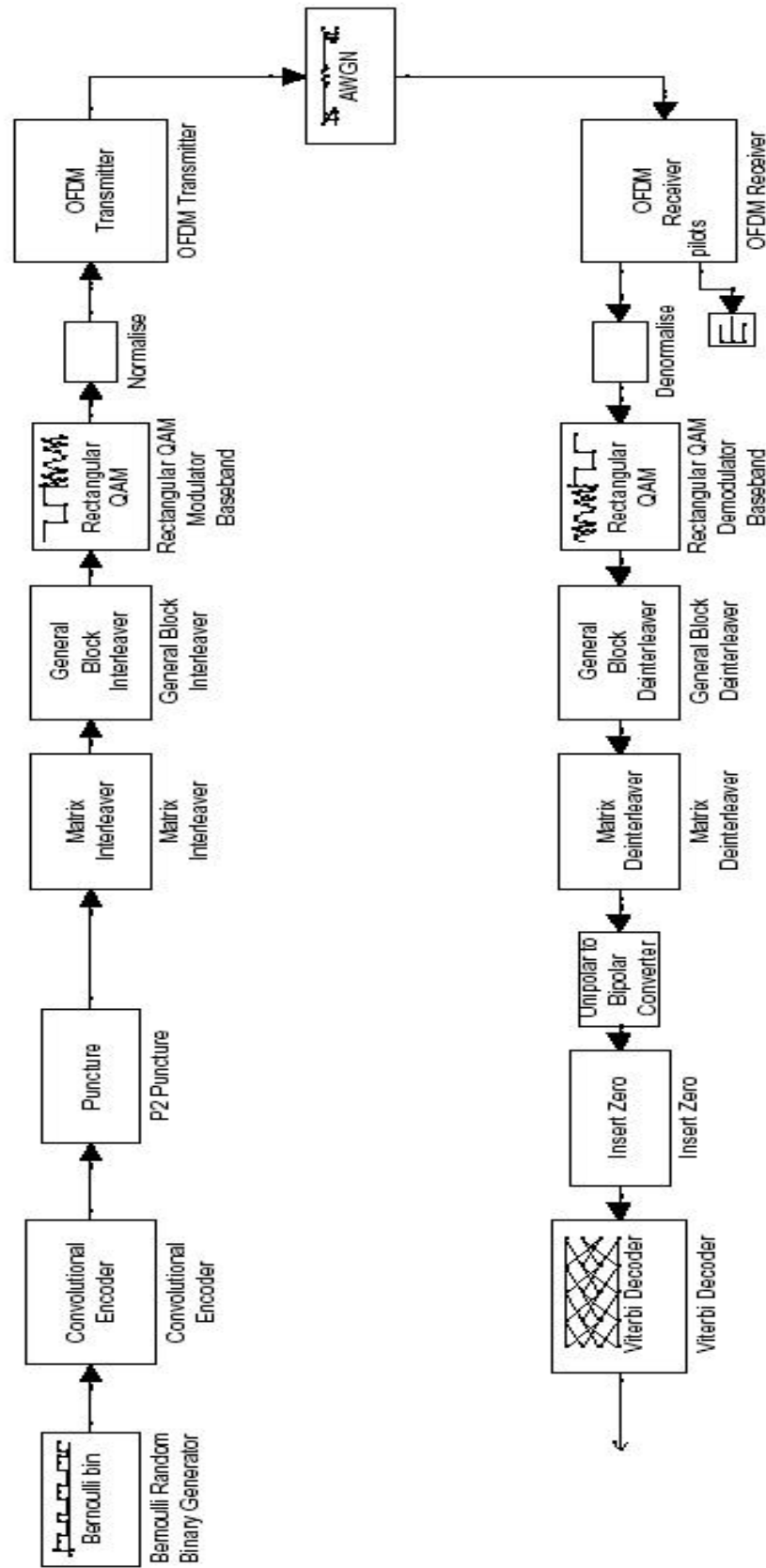


Fig 2.8 An example of practical OFDM system

Choosing communication hardware components with extremely broad linear range could mitigate this OOB power, but that would also badly decrease system efficiency, or introduce excess noise. Those drawbacks can be explained as follows.

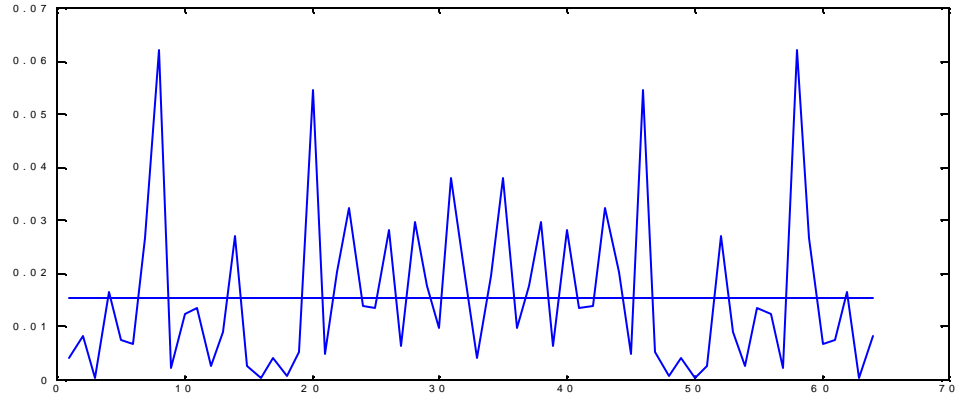


Fig.2.9 A PAPR example

Because of PAPR problem, a large dynamic range of the D/A and A/D converters will be required; otherwise, the peak values could be clipped, which would result in a signal distortion. On the other hand, if A/D and D/A converters with large working ranges are chosen, the quantization noise will increase and the system performance will degrade. In addition, the choices of power amplifier and up-converters will also be crucial when PAPR problem occurs. A large working range is required to ensure that the nonlinear distortion would not be introduced. As a result, power efficiency is decreased significantly due to PAPR problem. For example, the maximum power efficiency of a Class B power amplifier drops from 78.5% to 4.6%, when the PAPR increases 0dB to 17dB, as stated in the IEEE 802.11a standard. Power efficiency is pivotal in mobile communications such as laptop and PDA over the wired communications.

Since the PAPR problem is not the focus of this thesis, only an overview of existing solutions for PAPR is provided here. In fact, there are many approaches, such as

coding [17], partial transmit sequences [18], selective mapping [19], clipping [20], random phase updating algorithm [21], and sub-block phase weighting [22].

Chapter 3 Wireless Channel

In this chapter, four channel models are discussed, namely additive white Gaussian noise (AWGN) channel, Rayleigh channel, local model, and general multi-path fading with carrier frequency offset (CFO). In addition, the European COST 207 fading model is introduced.

3.1 AWGN and Fading Channel

The AWGN channel is the simplest channel model used in most communication systems. The thermal noise in the receivers can be characterized as an additive white Gaussian process. Although there are other factors inducing channel noise, such as antenna temperature, receiver filter, and multipath fading [23], only multipath fading will be studied in this chapter.

Channel fading is generally categorized into large-scale and small-scale fadings, which often occur simultaneously. Large-scale fading results from shadowing terrain contours such as hills, forests, or buildings, relative to the distance between transmitter and receiver. Small-scale fading, also known as Rayleigh fading, is not determined by the distance in communication. The small-scale fading is manifest in two ways: the signal spreading and the time variation.

3.2 Rayleigh Channel

A Rayleigh model is widely used to model wireless multipath fading channels in practice.

Rayleigh model is frequently used to describe a wireless channel with AWGN but without Light of Sign (LOS), where the power gain is subject to a random Rayleigh distribution. The complex channel impulse response $Y(t)$ can be given as:

$$Y(t) = g_i(t)\cos(\omega t + \mathbf{J}(t)) + jg_q(t)\sin(\omega t + \mathbf{J}(t)), \quad (3.2.1)$$

where g_i, g_q are Gaussian random variables, $\mathbf{J}(t)$ is uniformly distributed in $[0, 2\pi]$.

Then, the gain amplitude of the received signal can be expressed as:

$$g_r = \sqrt{g_i^2 + g_q^2} \quad (3.2.2)$$

It can be proved that g_r is a Rayleigh distribution as in Fig. 3.1, and its pdf is

$$p = \begin{cases} \frac{r}{s^2} \exp\left(-\frac{r^2}{2s^2}\right) & 0 \leq r < \infty \\ 0 & \text{otherwise} \end{cases} \quad (3.2.3)$$

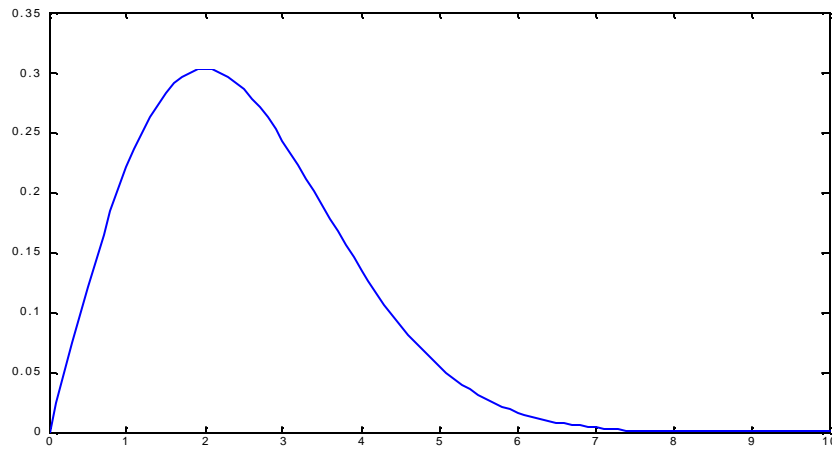


Fig. 3.1 Rayleigh distribution

According to the Jake's model [24], there are many transmission paths, and any of these path gains can be considered a Gaussian random variable. Then, the gross gain can be formulated as:

$$g_r = \sqrt{\sum_{l=0}^{M-1} g_l^2} \quad (3.2.4)$$

It has been proved that g_r is still a Rayleigh distributed process. However, when a LOS path exists, a Ricean model instead of a Rayleigh model should be considered.

3.3 Simple Local Model

A simple local model means that there is only a single path from the transmitter to the receiver. Some indoor environments can be modeled as simple local models, because their channel time delays are negligible. In such a circumstance, only carrier frequency offset needs to be considered.

According to Armstrong's OFDM channel analysis [25], a wireless channel can be characterized as a vector C , and the demodulated signal can be calculated by the convolution of C and the input data stream. It is noted that the white Gaussian noise is ignored in this model.

The vector C is defined as follows:

$$C = [c_0 \quad c_1 \quad c_2 \quad \cdots \quad c_{N-1}]$$

$$c_l = \frac{1}{N} \sum_{k=0}^{N-1} \exp\left(\frac{j2\pi k(l + e)}{N}\right)$$

$$= \frac{1}{N} \frac{\sin \mathbf{p}(l + \mathbf{e})}{\sin \mathbf{p}\left(\frac{l + \mathbf{e}}{N}\right)} \times \exp\left(j\mathbf{p} \frac{(N-1)(l + \mathbf{e})}{N}\right), \quad (3.3.1)$$

where \mathbf{e} is the normalized frequency offset and N is the IFFT length. If \mathbf{e} is zero in Eq. 3.3.1, which means that no CFO exists, $c_l = \mathbf{d}(l)$ results in no ICI. When CFO is present ($\mathbf{e} \neq 0$), $|c_l|$ will decrease as l increases. In other words, the intercarrier interference is caused mostly by neighboring subcarriers. This phenomenon is shown in Fig 3.2a.

Phases among subcarrier signals also vary in this model. We can approximate $\frac{N-1}{N}$ to 1 in Eq.3.3.1, when N is large. Then phases will change about \mathbf{p} from a subcarrier to next. Whenever l increments by 1, the sign of $\sin \mathbf{p}(l + \mathbf{e})$ will be inverted. In summary, the neighboring subcarriers have nearly the same phase, as illustrated in Fig.

3.2 b.

$$\text{Let } \mathbf{C} = \begin{bmatrix} c_0 & c_1 & \cdots & \cdots & c_{N-1} \\ c_{N-1} & c_0 & c_1 & \cdots & c_{N-2} \\ c_{N-2} & c_{N-1} & c_0 & \cdots & c_{N-3} \\ \vdots & \vdots & \vdots & \vdots & \vdots \\ c_1 & c_2 & \cdots & \cdots & c_0 \end{bmatrix}. \text{ Then the demodulated signal can be reformulated}$$

as $\mathbf{Y} = \mathbf{C}\mathbf{X}$;

3.4 COST 207 Fading Model

The COST 207 model was presented as an outdoor wireless channel model in Europe [27], which power gains, time delays, and Doppler spreading categories were specified for four typical environments.

These parameters were evaluated by numerous measurements performed in many countries, including the United Kingdom, France, and Sweden.

The four typical environments were rural area (RA), typical urban area (TU), bad urban area (BU), and hilly terrain (HT). COST 207 standard provided both the continuous time formula and discrete taps model.

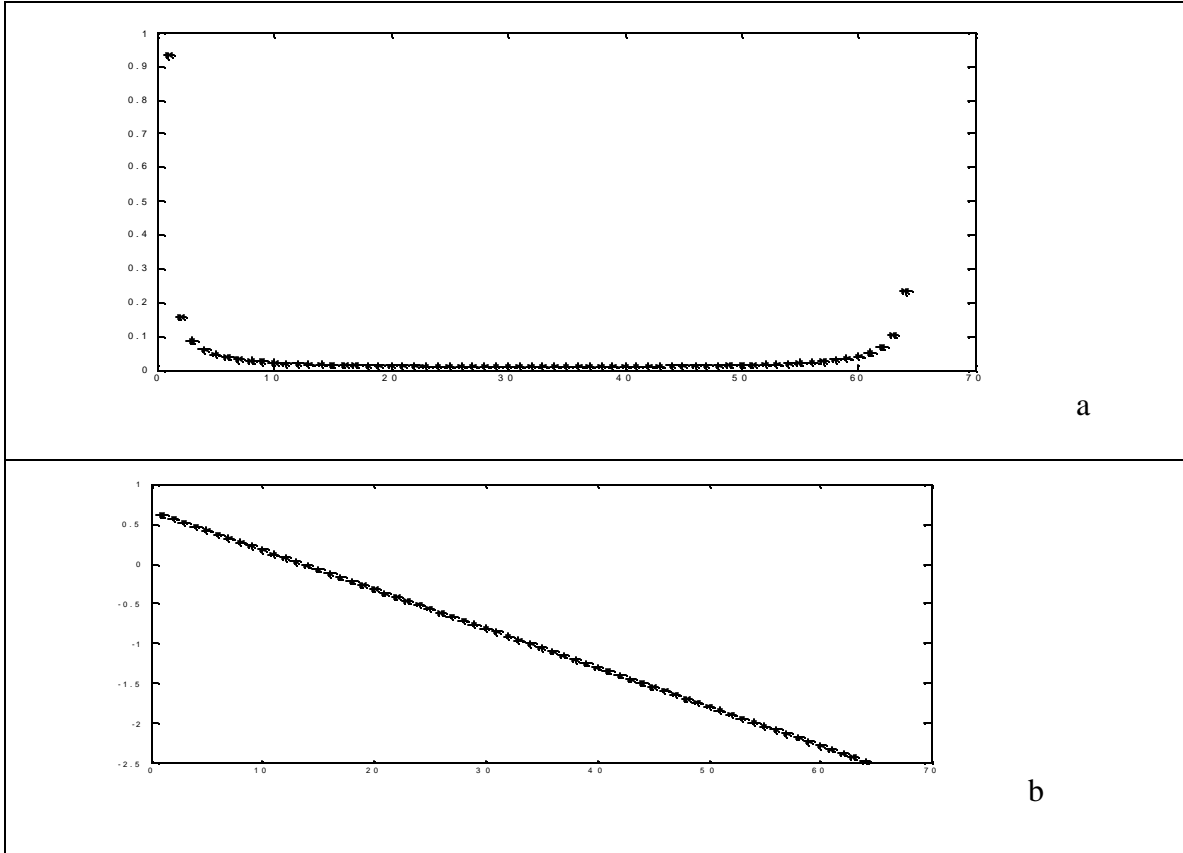


Fig 3.2 Amplitudes and phases of subcarriers. (N=64, CFO=0.2)

Their power distributions are characterized as follows:

RA:

$$P(t) = \begin{cases} \exp(-9.2t) & 0 \leq t \leq 0.7 \text{ ms} \\ 0 & \text{otherwise} \end{cases}$$

TU:

$$P(t) = \begin{cases} \exp(-t) & 0 \leq t \leq 7 \text{ ms} \\ 0 & \text{otherwise} \end{cases}$$

BU:

$$P(t) = \begin{cases} \exp(-9.2t) & 0 \leq t \leq 5 \text{ ms} \\ 0.5 \exp(5-t) & 5 \leq t \leq 10 \text{ ms} \\ 0 & \text{otherwise} \end{cases}$$

HT:

$$P(t) = \begin{cases} \exp(-3.5t) & 0 \leq t \leq 2 \text{ ms} \\ 0.1 \exp(15-t) & 15 \leq t \leq 20 \text{ ms} \\ 0 & \text{otherwise} \end{cases}$$

The COST-207 models are due to wide sense stationary uncorrelated scattering (WSSUS), with four types of Doppler spreading categories characterized by the maximum delays. Tapped delay-line models are often adopted to simplify the aforementioned continuous-time models. For example, the following table describes the tapped delay-line COST 207 RA model:

Table 3.1 COST207 RA tapped delay-line model

Tap number	1	2	3	4
Delay [us]	0	0.2	0.4	0.6
Power [dB]	0	-2	-10	-20
Doppler Category	RICE	Class	Class	Class

(RICE means Ricean distribution, while Class means classical (Jake) Doppler distribution in Table 3.1)

3.5 Multipath Fading with CFO

The channel is often modeled as a multipath fading in reality. Also, the COST207 models can be adopted to obtain multipath power gains and time delays for channel simulations. Different paths are represented as the taps in table 3.1, each path with a different power gain and a different time delay. The Doppler frequency shift and CFO are also considered in the channel simulations. A general multipath framework for all channel environments is designed, such environments including Rayleigh fading, simple local channel with CFO, COST 207 channels and so on.

The following symbols are used in the formulation of the general multipath framework.

Table 3.2 List of symbols

Symbol	Denotation	Note
N	Length of IFFT and FFT	In IEEE 802.11a 64
N_c	Length of Cyclic Prefix	In IEEE 802.11a 16
T	Duration of all N samples	In IEEE 802.11a 3.2 μs
f_c	Carry frequency	In IEEE 802.11a 5G
f_k	Sub-carrier's frequency space	In IEEE 802.11a 0.3125MHz
k	k^{th} sample in certain block	
i	i^{th} block, include N samples	
M	Number of paths	

p	p^{th} of M paths	
t_p	Time delay of p^{th} path	(table con'd)
Δf_p	Frequency offset of p^{th} path	
$a_{k,i}$	Input data	
$x(t)$	Output of IFFT	
$r(t)$	Received signal	
$y(t)$	Output of FFT	
$y_{l,i}$	l^{th} sample of i^{th} block	
$z_{m,i}$	m^{th} output of i^{th} block	

A pulse-shaping function can be defined as

$$P_T(t) = \begin{cases} 1 & 0 \leq t < 1 \\ 0 & \text{otherwise} \end{cases} \quad (3.5.1)$$

Other pulse-shaping waveforms such as raised-cosine function can also be applied [26]. The transmitted signal waveform consists of two parts. The first part is the OFDM modulated signal, and the second part is its cyclic extension. It is assumed that the first block of data can achieve perfect time synchronization. Under the assumption that the power amplifier and antenna is ideal, the OFDM modulated signal with CP is exactly the signal in the air.

Suppose there are M paths, and each path has different gain, time delay, and frequency offset. Then, the received signal can be written as:

$$r(t) = \sum_{p=1}^M g_p x(t - \mathbf{t}_p, f_c + \Delta f_p), \quad (3.5.2)$$

where $x(t)$ is the transmitted signal. Then, the received $r(t)$ will be down-converted to form a baseband signal $y(t)$.

Define $L_c = \frac{N_c}{N}$, then

$$y(t) = r(t) \exp[-j2\pi f_c (t - i(1 + L_c)T)] , \quad (3.5.3)$$

where $r(t)$ is as in Eq. 3.5.2

In addition, the low pass filter is assumed to be ideal, and no aliasing is introduced here. Substituting Eq. 3.5.2 into the equation 3.5.3, then, sampling $y(t)$ at the time instants as follows:

$$t = i(1 + L_c)T + l \frac{T}{N} . \quad (3.5.4)$$

Then, the discrete-time data stream $y_{l,i}$ will be sent for FFT operation. The output of the FFT can be written:

$$z_{m,i} = \frac{1}{N} \sum_{l=0}^{N-1} y_{l+N_c,i} \exp\left(-2\pi j l \frac{m}{N}\right) \quad (3.5.5)$$

Eq. 3.5.5 can be simplified as:

$$z_{m,i} = \sum_{k=0}^{N-1} a_{k,i} c_{k,l,m} \quad (3.5.6)$$

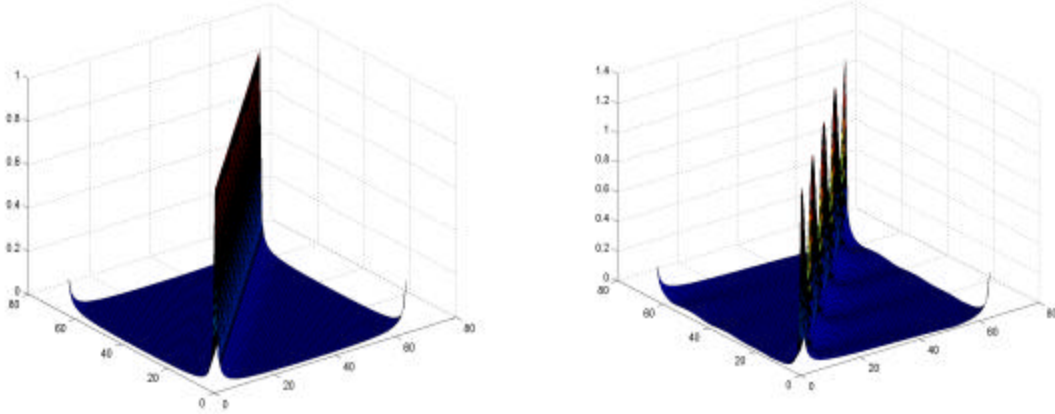
Generally, it can be divided into two parts, the signal part and the interference part, and it can be rewritten as follows:

$$z_{m,i} = a_{m,i} c_{m,l,m} + \sum_{k \neq m} a_{k,i} c_{k,l,m} , \quad (3.5.7)$$

where $c_{k,l,m}$ is defined as:

$$\begin{aligned}
c_{k,l,m} = & \frac{1}{N} \sum_{p=1}^M g_p \sum_{i=0}^{N-1} \exp \left[-2\mathbf{p}j \left(f_c L_c T + f_c \mathbf{t}_p + \Delta f_p \mathbf{t}_p - k \frac{\mathbf{t}_p}{T} \right) \right] \exp \left(\frac{2\mathbf{p}j(k-m+\Delta f_p T)l}{N} \right) \\
& \times P_T \left(\frac{lT - N\mathbf{t}_p}{NT} \right) \\
& + \frac{1}{N} \sum_{p=1}^M g_p \sum_{i=0}^{N-1} \exp \left[2\mathbf{p}j \left(f_c (1-L_c)T - f_c \mathbf{t}_p + \Delta f_p (T-\mathbf{t}_p) - k \frac{\mathbf{t}_p}{T} \right) \right] \\
& \times \exp \left(\frac{2\mathbf{p}j(k-m+\Delta f_p T)l}{N} \right) \times P_T \left(\frac{lT + NL_c T - N\mathbf{t}_p}{NL_c T} \right). \tag{3.5.8}
\end{aligned}$$

Since $c_{k,l,m}$ depends on $k-m$, and l only, it is noted that $c_{k,l,m} = f(i, l)$ can be stated, where $i = k-m$ in Eq. 3.5.8. Compared with the simple local model where any row in the matrix can be determined by a cyclic shift of the first row, the new channel model doesn't have such a cyclic structure. This difference is shown in Fig 3.3.



a. Local simple model

b. multipath fading model

Fig. 3.3 Two Channel Models (N=64, CFO=0.2)

In the Fig.3.3 b, even though the peak values of subcarriers are different, the following rules still hold: first, the peak values always occur at diagonal locations; second, interference is mostly due to the neighboring subcarriers.

A Fourier transform matrix can be defined as:

$$F = \begin{bmatrix} 1 & 1 & \cdots & 1 \\ 1 & e^{jw} & & e^{jw(N-1)} \\ \vdots & & & \\ 1 & e^{jw(N-1)} & & e^{jw(N-1)^2} \end{bmatrix}, \quad (3.5.9)$$

where $w = \frac{2p}{N}$.

The signal source vector is denoted as $S = [s_0 \ s_1 \ \cdots \ s_{N-1}]^T$.

Then the IFFT-modulated signal vector can be written as:

$$X = F^* S, \quad (3.5.10)$$

where F^* is the complex conjugate of matrix F .

Let the channel impulse response be $h(l)$. The received signal vector Y can be formulated as

$$Y = X \otimes h(l). \quad (3.5.11)$$

After down-conversion, where the CFO needs to be considered, the FFT-demodulated signal can be written as,

$$R = F(EY), \quad (3.5.12)$$

where $E = \text{diag}([1, e^{je}, e^{2je}, \dots, e^{j(N-1)e}])$.

Finally, the received signal vector R can be expressed as follows:

$$R = FEF^* HS + FN_{AWGN}, \quad (3.5.13)$$

where $H = \text{diag}(\text{fft}(h(l), N))$, is the frequency response of the channel; and N_{AWGN} is the white noise

Chapter 4 Inter-carrier Interference Problem and Solutions

Inter-carriers interference (ICI) is a special problem in the OFDM system. In this chapter, the factors inducing ICI and the solutions will be investigated.

4.1 Factors Inducing ICI

ICI is different from the co-channel interference in MIMO systems. The co-channel interference is caused by reused channels in other cells [28], while ICI results from the other sub-channels in the same data block of the same user. Even if only one user is in communication, ICI might occur, yet the co-channel interference will not happen. There are two factors that cause the ICI, namely frequency offset and time variation. As discussed in [29], some kinds of time variations of channels can be modeled as a white Gaussian random noise when N is large enough, while other time variations can be modeled as frequency offsets, such as Doppler shift. Only frequency-offset is discussed in this chapter. ICI problem would become more complicated when the multipath fading is present. The following figure shows the relationship between CFO and ICI.

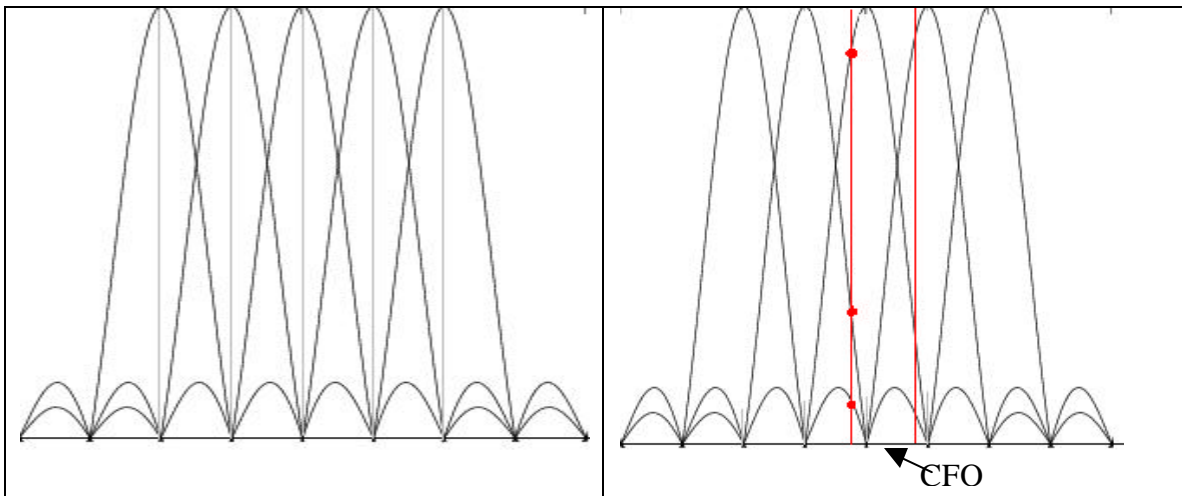


Fig. 4-1. Relationship of CFO and ICI.

A. Doppler Effect:

The relative motion between receiver and transmitter, or mobile medium among them, would result in the Doppler effect, a frequency shift in narrow-band communications. For example, the Doppler effect would influence the quality of a cell phone conversation in a moving car.

In general, the Doppler frequency shift can be formulated in a function of the relative velocity, the angle between the velocity direction and the communication link, and the carrier frequency, as shown in Fig. 4.2

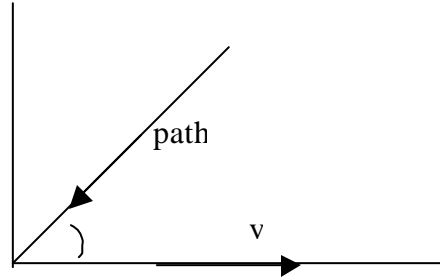


Fig. 4.2 Doppler Effect

The value of Doppler shift could be given as

$$f_d = \frac{v}{\lambda} 2\pi \cos(q), \quad (4.1.1)$$

where q is the angle between the velocity and the communication link, which is generally modeled as a uniform distribution between 0 and 2π , v is the receiver velocity, and the λ is the carrier wavelength.

Let us assume that electromagnetic wave velocity is C , the wavelength of carrier can be written as

$$\lambda = \frac{C}{f_c}, \quad (4.1.2)$$

where f_c is the carrier frequency.

Three kinds of Doppler effect models are generally discussed in existing literatures: the classical model, the uniform model, and the two-ray model. The classical model is also referred as Jake model, which was proposed in 1968 [24]. In this model, the transmitter was assumed to be fixed with vertically polarized antenna. There was no Line of Sight (NLOS) path, and all path gains were subject to identical statistics. It had been proved in 1972 [16] that the spectrum of this kind of Doppler shift could be given as:

$$P_J(f) = \frac{k}{2f_m \sqrt{1 - \left(\frac{f - f_c}{f_m}\right)^2}}, \quad (4.1.3)$$

where k was fixed constant to given channel and antenna, f_m was the maximum Doppler shift as in Eq. 4.1.1 and f_c was defined in Eq. 4.1.2.

The uniform model is much simpler. Both velocity and angle are supposed to be uniformly distributed [30]. In this case, the power spectrum could be written as:

$$P_U(f) = \begin{cases} \frac{1}{2f_d} & |f| \leq f_d \\ 0 & \text{otherwise} \end{cases} \quad (4.1.4)$$

The two-ray model assumed that there were only two paths between the transmitter and receiver. Accordingly, the resulting power spectrum is given as [30]

$$P_T(f) = \frac{1}{2} [\mathbf{d}(f - f_d) + \mathbf{d}(f + f_d)] \quad (4.1.5)$$

B. Synchronization Error

It can be assumed that most of the wireless receivers cannot make perfect frequency synchronization. In fact, practical oscillators for synchronization are usually

unstable, which introduce frequency offset. Although this small offset is negligible in traditional communication systems, it is a severe problem in the OFDM systems. In most situations, the oscillator frequency offset varies from 20 ppm (Parts Per Million) to 100 ppm [31]. Provided an OFDM system operates at 5 GHz, the maximum offset would be 100 KHz to 500 KHz (20-100 ppm.). However, the subcarriers frequency spacing is only 312.5 KHz. Hence; the frequency offset could not be ignored.

In most literatures, the frequency offset can be normalized by the reciprocal of symbol duration. For example, if a system has a bandwidth of 10 MHz, and the number of subcarriers is 128, then the subcarrier frequency spacing would be $10\text{M}/128 = 78\text{ KHz}$. If the receiver frequency offset is 1 KHz, then the normalized frequency offset will be $1/78 = 1.3\%$. If the normalized frequency offset is larger than 1, only the decimal part needs to be considered, as shown in Fig. 4.1.

C. Multipath Fading

The influence of multipath fading on ICI is seldom discussed before. As a matter of fact, the multipath fading does not cause ICI, but it will make the ICI problem worse. Since ICI cannot be neglected in practice, the impact of multipath fading should be discussed. It is recognized that the cyclic prefix has been used to eliminate ISI entirely and therefore only ICI needs to be concerned. Because there are many time-delayed versions of received signals with different gains and different phase offsets, the ICI is more complicated to calculate.

There are many multipath channel models. Even in the European COST 207 standard, there are four different typical models. In addition, Rayleigh and Rician channels could also be considered as multipath models.

4.2 Intercarrier Interference and Signal-to-interference Ratio

As mentioned in Chapter 3, the channel can be expressed as a matrix C . The received signal can therefore be written as:

$$Y = CS + N_w, \quad (4.2.1)$$

where S is the $N \times M$ input data, M is the number of blocks, each block consists of N input bits, and N_w is the white noise. Noise components will not be discussed and then will be neglected from now on. Ideally, C is an $N \times N$ identity matrix. However, with the existence of CFO, the matrix has nontrivial off-diagonal elements. Hence, Eq. 4.2.1 could be rewritten as:

$$Y(k) = S(k)C_{kk} + \sum_{l \neq k} S(l)C_{kl} \quad (4.2.2)$$

The first part in Eq. 4.2.2 consists of the information-bearing signals, while the second part is intercarrier interference.

However, C will be different in simple local models and multipath models.

A. ICI in Simple Local Model

In this case, the matrix C is cyclic as follows:

$$C = \begin{bmatrix} C_0 & C_1 & \cdots & \cdots & C_{N-1} \\ C_{N-1} & C_0 & C_1 & \cdots & C_{N-2} \\ C_{N-2} & C_{N-1} & C_0 & \cdots & C_{N-3} \\ \vdots & \vdots & \vdots & \vdots & \vdots \\ C_1 & C_2 & \cdots & \cdots & C_0 \end{bmatrix}$$

In other words, all sub-channels can be characterized by the same impulse response.

And the entries of the complex matrix C can be written as in [32]. This formula is also showed in Chapter 3.

$$C_i = \frac{\sin(\mathbf{p}(i + \mathbf{e}))}{\sin\left(\frac{\mathbf{p}(i + \mathbf{e})}{N}\right)} \exp\left(\frac{j\mathbf{p}(N-1)(i + \mathbf{e})}{N}\right), \quad (4.2.3)$$

where \mathbf{e} is the normalized frequency offset and N is IFFT length.

Then, Eq. 4.2.2 can be rewritten as:

$$Y(k) = S(k)C_0 + \sum_{l=1}^{N-1} S(l)C_{l-k}. \quad (4.2.4)$$

B. ICI in Multipath Model

The ICI in multipath model is more complicated, as shown in Chapter 3. We just rewrite the equation here.

$$\begin{aligned} c_{k,l,m} = & \frac{1}{N} \sum_{p=1}^M g_p \sum_{i=0}^{N-1} \exp\left[-2\pi j \left(f_c L_c T + f_c \tau_p + \Delta f_p \tau_p - k \frac{\tau_p}{T} \right)\right] \exp\left(\frac{2\pi j (k - m + \Delta f_p T)}{N}\right) \\ & \times P_T\left(\frac{IT - N\tau_p}{NT}\right) \\ & + \frac{1}{N} \sum_{p=1}^M g_p \sum_{i=0}^{N-1} \exp\left[2\pi j \left(f_c (1 - L_c) T - f_c \tau_p + \Delta f_p (T - \tau_p) - k \frac{\tau_p}{T} \right)\right] \\ & \exp\left(\frac{2\pi j (k - m + \Delta f_p T)}{N}\right) \times P_T\left(\frac{IT + NL_c T - N\tau_p}{NL_c T}\right) \end{aligned} \quad (4.2.5)$$

In this equation, power gains subcarrier-dependent. In other words, different subcarriers have different power gains. C is not a simple cyclic matrix here as that in the simple model.

C. Signal to Interference Ratio

The signal to interference ratio (SIR) measure is often quantify ICI. For a simple channel model, SIR can be written as Eq. 4.2.6:

$$SIR_c = \frac{|C_0|^2}{\sum_{i=1}^{N-1} |C_i|^2} \quad (4.2.6)$$

In a multipath case, SIR of the L^{th} sub-channels is given as:

$$SIR_L = \frac{|C_{LL}|^2}{\sum_{\substack{i=0 \\ i \neq L}}^{N-1} |C_{Li}|^2}, \quad L = 0, 1, 2, \dots, N-1 \quad (4.2.7)$$

The overall SIR of all sub-channels can be defined as $SIR_w = E(SIR_L)$.

4.3 Solutions for ICI

Many existing scheme were proposed to attack ICI problem. Three kinds of approaches are addressed here. The first approach is based on CFO estimation and compensation, which makes use of pilot sequences, virtual carriers or blind signal processing techniques. The second approach is based on the windowing technique in either time domain or frequency domain, such as Nyquist windowing and Hanning windowing. The third one is called ICI self-cancellation, or Polynomial cancellation coded (PCC), where the repeated bits are transmitted to mitigate inter-carrier interference.

A. CFO Estimation

In order to compensate CFO, CFO must be estimated at first. Once a precise CFO estimate is obtained, a perfect equalizer then can be designed to eliminate ICI.

Signal processing methods are applied to solve this problem. Liu and Tureli proposed MUSIC-based and ESPRIT-based algorithms to estimate CFO [33]. Basically, their methods are non-blind because they used virtual carriers, just as in [34, 35]. Other

researchers proposed Maximum Likelihood for CFO estimation [36], which was proved to be equivalent to Music-based algorithm. Other CFO estimation methods involve with training sequences [37].

B. Windowing

Fig. 4.4 shows the OFDM transmitter structure with the windowing technique, while the receiver remains the same as the principal OFDM receiver. It is well known that the multiplication operation in the frequency domain is equivalent to the circular convolution in the time domain. Different windowing by choosing parameters w_i can result in different digital filtering.

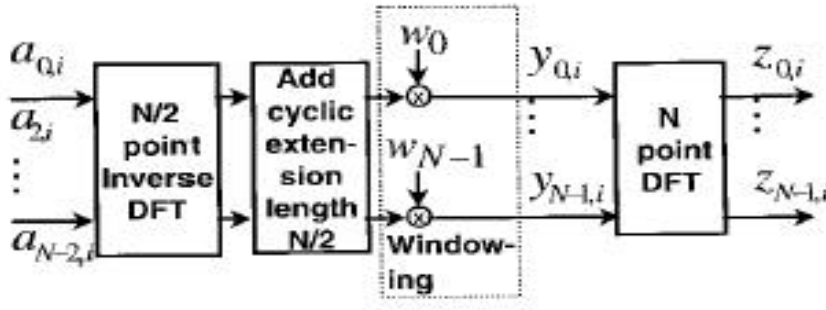


Fig. 4.4 Windowing in the transmitter.

As stated in [25], there are many kinds of windowing schemes to reduce the ICI due to CFO, such as the Hanning window, the Nyquist window, and the Kaiser window. In [38], the MMSE Nyquist window is used to mitigate the white noise.

C. Intercarrier Interference Self-cancellation

The ICI self-cancellation scheme is a method involving with encoded redundancy. Compared with other schemes, only half or less of bandwidth is used for information transmission. In other words, only half or less of full data rate could be achieved. Same bandwidth efficiency will be achieved for ICI self-cancellation and $\frac{1}{2}$ -rate convolution

coding. However, empirical results have shown that ICI self-cancellation outperforms the convolution coding in most channel environments.

The redundant information in an ICI self-cancellation encoder can be applied to eliminate the ICI at the receiver. The principles of ICI self-cancellation can be illustrated in Fig 4.5.

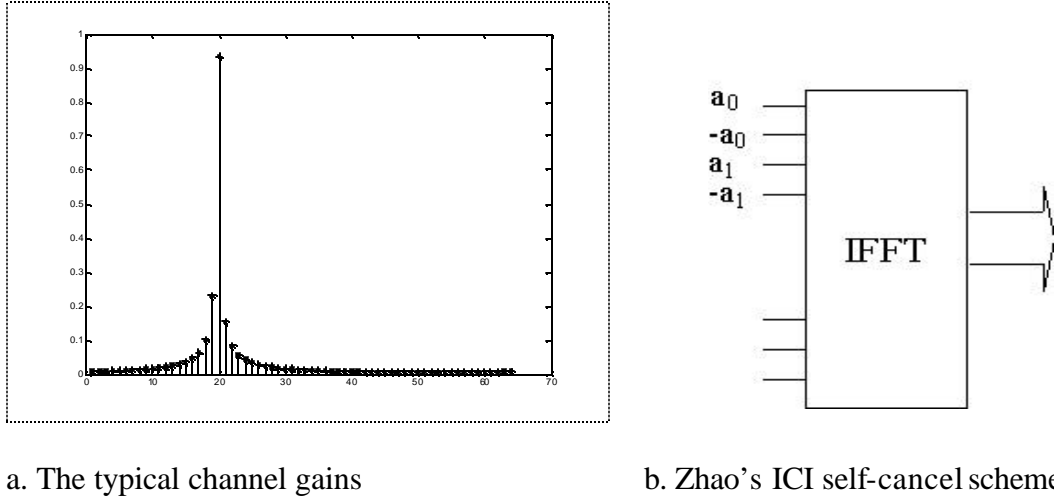


Fig. 4.5 Self-cancellation example

As shown in Fig. 4.5 (a), only the first and second subcarriers have a large gain difference. The difference between any other neighboring subcarriers is much smaller. The $(l+1)^{th}$ subcarrier carries the inverted signal as the l^{th} subcarrier does. The intercarrier interference from l^{th} , and $(l+1)^{th}$ subcarriers can cancel each other. This is the key idea for the ICI self-cancellation schemes.

Armstrong extended the original ICI self-cancellation encoder to any larger amount of redundant repetitions. This new scheme was also referred as Polynomial Cancellation Coded (PCC) scheme. Another ICI self-cancellation scheme is proposed recently [39]. In

this new scheme, a different bit encoder is applied, and it will result in a better performance in certain channel models than the PCC scheme.

In the next chapter, this scheme will be discussed in detail.

Chapter 5 Clustering Detection and Multiple Codebook

In this chapter, two kinds of intercarrier interference (ICI) self-cancellation schemes will be discussed. First a clustering procedure is applied to improve OFDM signal detection. Then a general coding framework for ICI self-cancellation schemes will be introduced. Finally a summary of this thesis and future research plan will be addressed.

5.1 Clustering Intercarrier Interference Cancellation

A. Justification of Slowly Time-varying

The clustering scheme is based on the assumption that the wireless channel is a slow-fading channel, that will be locally time-invariant among a few blocks, as recognized in many literatures, such as in [30, 40, 41]. It can be manifested in the following justifications.

The definition of slow fading is $T_c \gg T_s$, where T_c is the coherent time and T_s is the symbol duration. T_c is the parameter used to characterize the time-varying nature of the Doppler effect. Generally, T_c is defined as

$$T_c = \sqrt{\frac{9}{16pf_m}}, \quad (5.1.1)$$

where f_m is the maximum of Doppler frequency shift, which can be obtained through the following equation:

$$f_m = \frac{v_m}{\lambda_c} = \frac{v_m f_c}{c}, \quad (5.1.2)$$

where v_m is the maximum velocity, f_c is the carrier frequency, and c is the speed of light. The coherent time T_c can be calculated as

$$T_c = \sqrt{\frac{9c}{16\mathbf{p}v_m f_c}} . \quad (5.1.3)$$

B. Clustering Method

The central idea for the clustering technique is that all subcarriers have almost identical phase offsets. This is valid because all subcarriers travel through the same paths. Also, suppose that the noise is white Gaussian noise.

Because the data sent is from a finite alphabet set, such as BPSK, QPSK and QAM, the received signals will scatter around such a finite alphabet set, as depicted in Fig 5.1.

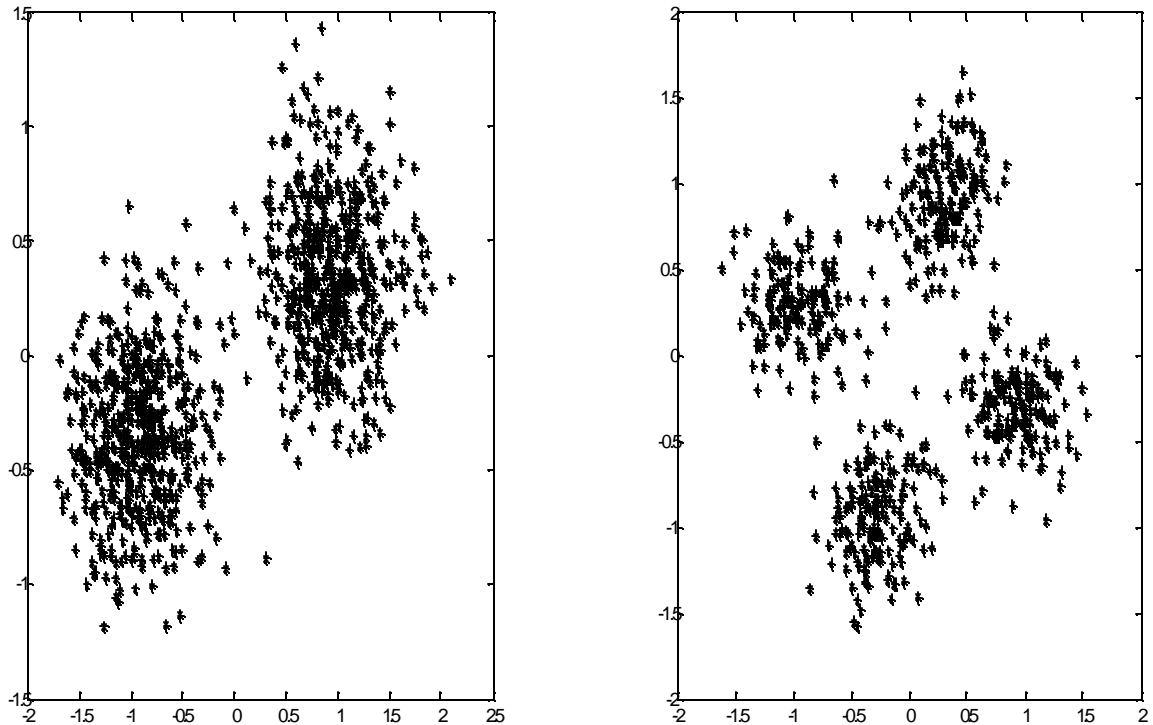


Fig 5.1 a Received BPSK signals

b. Received QPSK signals

C. Pilot Bits

In IEEE 802.11a, there are four sub-carriers reserved for pilot bits. However, in our scheme, only two pilot subcarriers are requested. Based on the received pilot signals, the channel gains can be estimated

D. Simulation Results

The previous ICI self-cancellation scheme, convolution coding, normal (without convolution coding and self-cancellation), and ICI self-cancellation with clustering are compared in Figure 5.2. Fig. 5.2 shows that bit error rates versus the signal-to-noise ratios for different OFDM schemes.

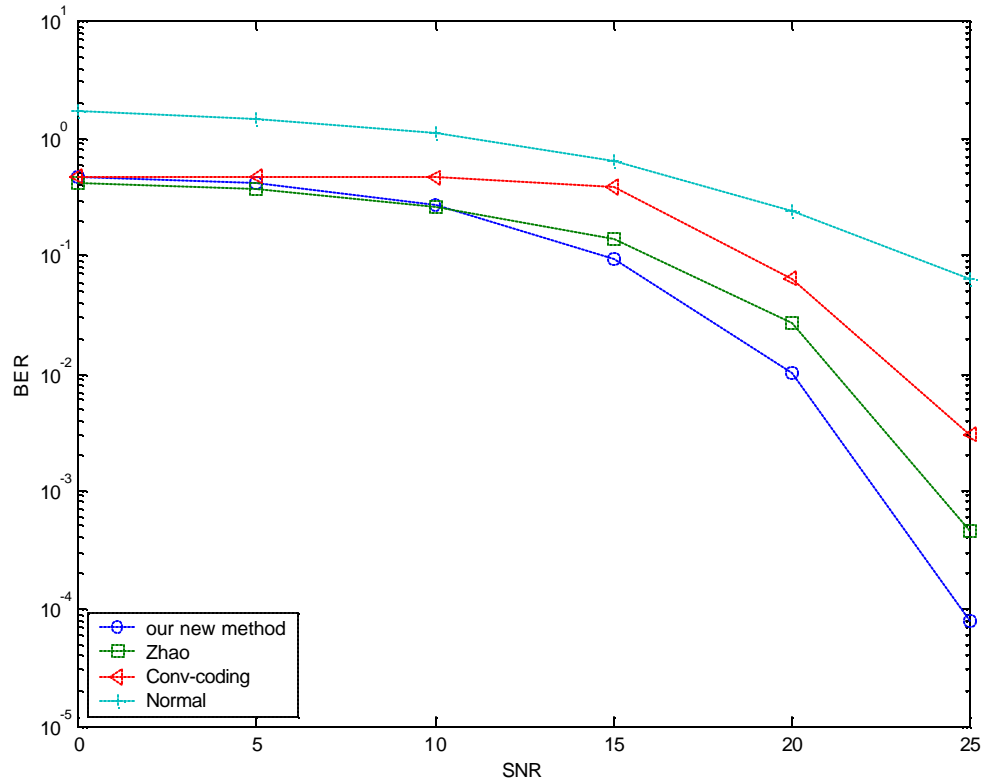


Fig. 5.2. Simulation results of local model, CFO=0.2

The number of subcarriers is 256, and the CFO is 0.2. The convolution coding in the industrial standard is used in these simulations ($g_0 = 133_8$ and $g_1 = 171_8$ rate = 1/2). The standard Viterbi hard-decision decoder is applied at the receiver. Obviously, the new scheme outperforms other existing schemes. The Fig 5.3 shows the results for $CFO=0.15$, COST 207 channel model in rural areas. In both simulations, 2000 Monte Carlo trials are taken.

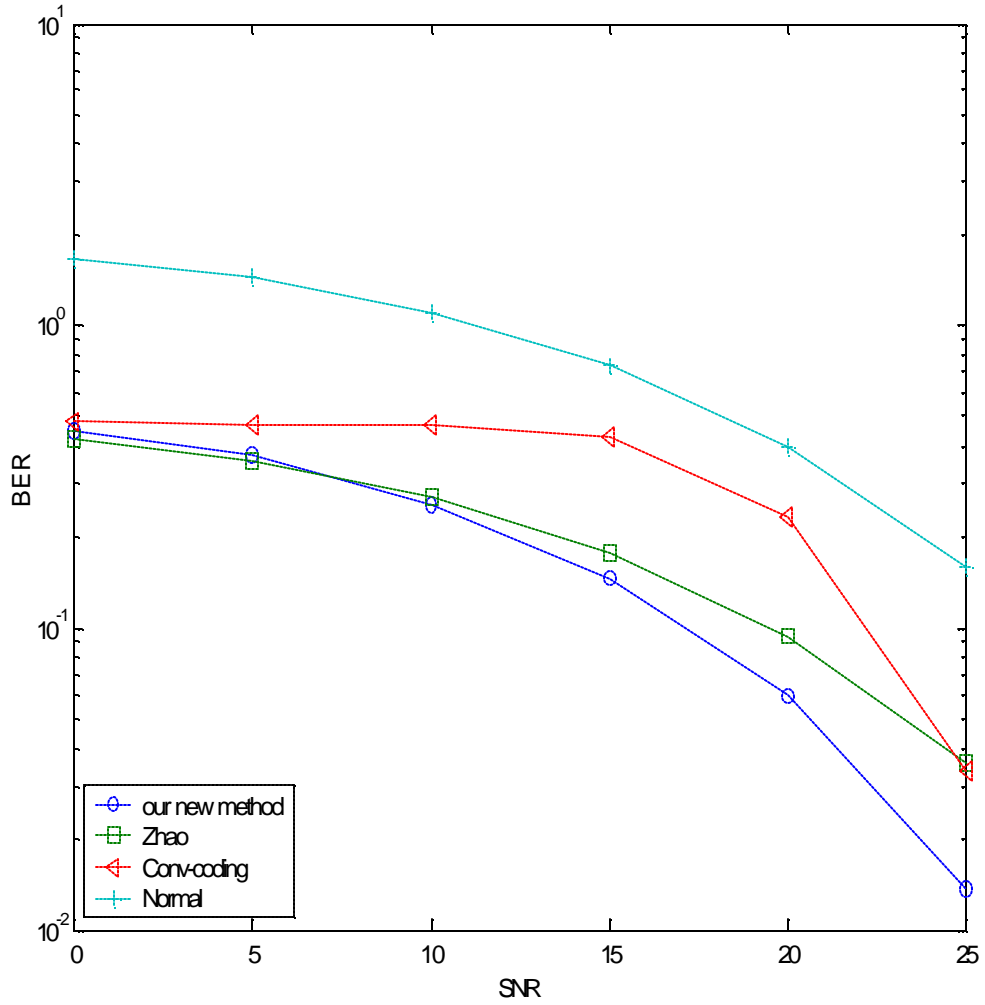


Fig. 5.3 Simulation of Multipath model. CFO=0.15

5.2 Multiple-Codebook

A general framework of ICI self-cancellation is presented here. Such a new framework will include not only the existing ICI self-cancellation codebooks but also new potential codebooks.

A. General Structure of ICI Self-cancellation

A precoder H of a matrix form, can be design as depicted in Fig. 5.4. Since the ICI self-cancellation encoder inserts as many redundant bits as the information bits, the function of H can be written as a $N \times \frac{N}{2}$ matrix.

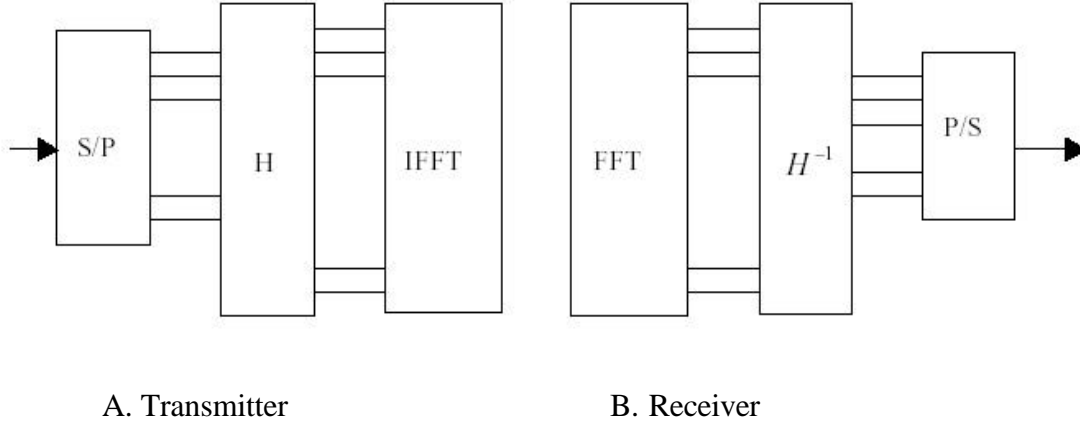


Fig 5.4 Simplified block diagram of ICI self-cancellation scheme

An example of H is as follows. Supposedly, the information bit vector is $S = [s_1 \ s_2 \ s_3 \ \cdots \ s_{N/2}]^T$. This vector can be obtained from the serial-to-parallel component as in Fig 5.4. The length of S is $N/2$ in this situation.

Even only the one-time repeating schemes (rate is $1/2$) will be discussed here, it can be automatically extend to higher repeating schemes.

$$H_1 = \begin{bmatrix} 1 & 0 & \cdots & 0 \\ -1 & 0 & \cdots & 0 \\ 0 & 1 & 0 & \vdots \\ 0 & -1 & 0 & 0 \\ 0 & 0 & \ddots & 0 \\ \vdots & 0 & \ddots & 0 \\ \vdots & \vdots & 0 & 1 \\ 0 & \cdots & 0 & -1 \end{bmatrix}$$

Then, according to Zhao's ICI self-cancellation encoder, the OFDM-modulated signal will be $H_1 S = [s_1 \quad -s_1 \quad s_2 \quad -s_2 \quad s_s \quad \cdots \quad -s_{N/2}]^T$ [32]. Similarly, Sathananthan proposed another ICI self-cancellation encoder H_2 as follows:

$$H_2 = \begin{bmatrix} 1 & 0 & \cdots & 0 \\ 0 & 1 & \cdots & 0 \\ 0 & 0 & \ddots & \vdots \\ \vdots & 0 & 0 & 1 \\ \vdots & \vdots & 0 & -1 \\ \vdots & 0 & \ddots & 0 \\ 0 & -1 & 0 & \vdots \\ -1 & 0 & \cdots & 0 \end{bmatrix}$$

In this scheme, the OFDM-modulated signal will be $[s_1 \quad s_2 \quad s_3 \quad \cdots \quad -s_3 \quad -s_2 \quad -s_1]^T$ as in [39]. A $(2M \times M)$ matrix H_s is defined as a sub-block in the codebook H , where M is the number of columns in H_s . It can be written as

$$H_s = \begin{bmatrix} I_{M \times M} \\ -\Psi_{M \times M} \end{bmatrix}, \quad (5.2.1)$$

where $\mathbf{Y}_{M \times M} = \begin{bmatrix} 0 & \cdots & 0 & 1 \\ \vdots & & \ddots & 0 \\ 0 & 1 & & \vdots \\ 1 & 0 & \cdots & 0 \end{bmatrix}_{M \times M}$ and $I_{M \times M}$ is an $M \times M$ identity matrix. The

parameter M could be chosen according to:

$$M = 2^k \quad k = 0, 1, \dots, \log_2 \left(\frac{N}{2} \right) \quad (5.2.2)$$

Then we can create a codebook H from based on H_s as follows:

$$H_i = \begin{bmatrix} H_s & & & O \\ & H_s & & \\ & & \ddots & \\ O & & & H_s \end{bmatrix} \quad (5.2.3)$$

When we set $k = \log_2 \left(\frac{N}{2} \right)$, then $M = \frac{N}{2}$ and we obtain the codebook H_2 . On the other hand, H_1 can be generated by choosing $k = 0$.

If we choose different k , such as $k = 2, 4, \dots$, other kinds of codebooks H can be obtained, resulting in multiple codebooks.

B. Comparison of Codebooks

It is necessary to compare these ICI self-cancellation codebooks among different environments, such as local channel with different CFO, Rayleigh channel, multipath fading channel with CFO.

In a simple local model, all codebooks show similar in performance, although Zhao's scheme is better when the CFO is small.

When the CFO is as large as 0.4, all of the schemes demonstrate poor performance. Fig 5.5 provides simulation results for CFO=0.3.

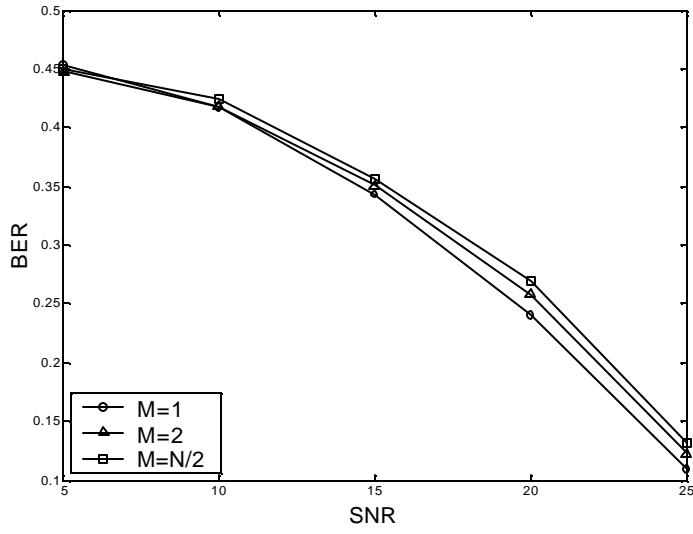


Fig. 5.5 Multi-codebooks for simple local model CFO=0.3

For Rayleigh Channels, all ICI self-cancellation schemes have similar performances. However, Zhao's codebook is slightly better than others when the SNR is low.

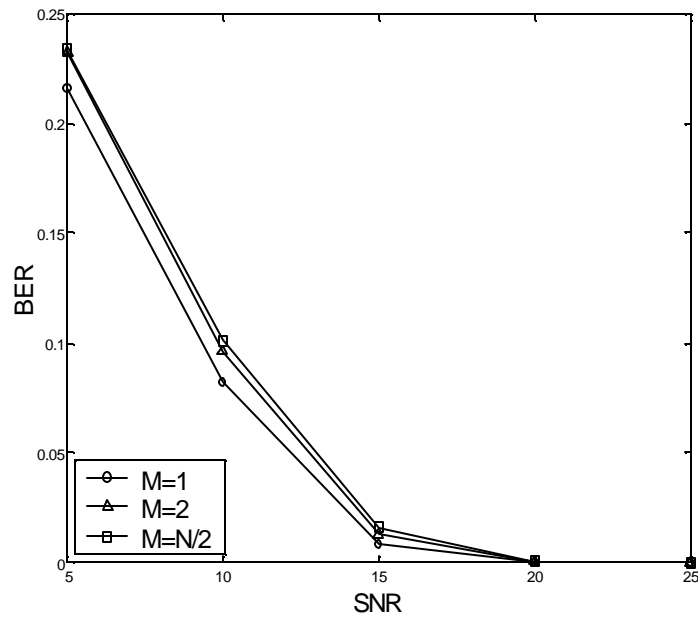


Fig 5.6 Multi-codebooks for Rayleigh channels

For multipath fading models, such as COST 207 RA model, Sathananthan's scheme is better when CFO is large. However, when CFO decreases down to 0.05, a new codebook becomes the best among multiple codebooks, as shown in Fig. 5.7:

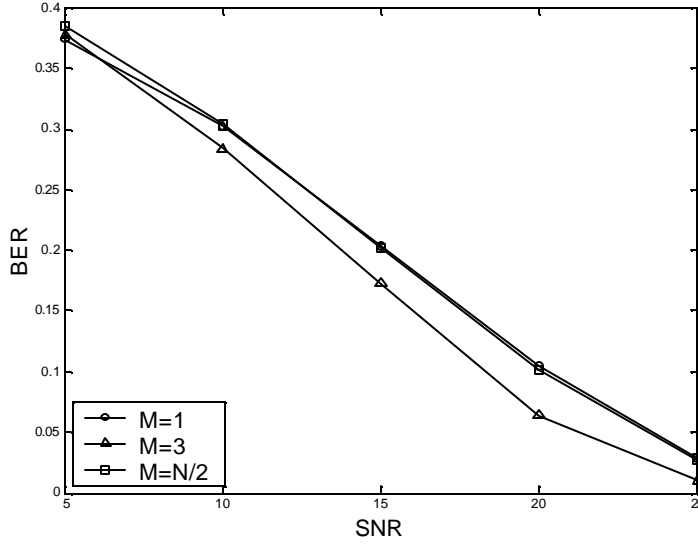


Fig 5.7 Multiple-Codebooks for Multipath channel. CFO=0.05

5.3 Summary and Further Work

Since the clustering scheme greatly improved the ICI self-cancellation receivers, and the multi-codebooks will show robust performance among different channel environments, it is desirable to investigate a hybrid system integrating these two methods in a variety of environments, such as the Rayleigh channel, or the MIMO fading. Another extension would be combining the ICI self-cancellation scheme with error control codes and RAKE receivers to achieve yet-better OFDM performance.

In addition, new techniques would be investigated in the future such as in [42,44].

References

- [1] R.W. Chang, "Synthesis of band- limited orthogonal signals for multichannel data transmission," Bell Sys. Tech. Journal, vol. 45, Dec. 1966
- [2] Zou, W.Y. and Yiyan Wu, "COFDM: an overview" IEEE Trans. on Broadcasting, vol. 41 Issue: 1, pp. 1-8, Mar. 1995
- [3] Weinstein, S. and Ebert, P.; "Data Transmission by Frequency-Division Multiplexing Using the Discrete Fourier Transform" IEEE Trans. on Commun. vol. 19 Issue: 5, pp. 628 –634, Oct.1971
- [4] Peled, A. and Ruiz, A.; "Frequency domain data transmission using reduced computational complexity algorithms", Acoustics, Speech, and Signal Processing, IEEE International Conference on ICASSP '80, vol. 5, pp.964 –967, Apr. 1980
- [5] B. Hirosaki, "An analysis of automatic equalizers for orthogonally multiplexed QAM systems," IEEE Trans. Commun. , vol. COM-28, pp.73-83, Jan.1980.
- [6] L.J. Cimini, "Analysis and simulation of a digital mobile channel using orthogonal frequency division multiplexing", IEEE Trans. Commun. , vol. COM-33, pp. 665-675. July 1985
- [7] I. Kalet, "The multitone channel," IEEE Trans. Commun. vol. 37, pp.119-124. Feb.1989
- [8] http://www.dvb.org/dvb_technology/whitepaper-pdf-docs/dvbtpaper.pdf
- [9] <http://idec.chonnam.ac.kr/data/2001/remo/9.26/4.pdf>
- [10] <http://standards.ieee.org/getieee802/802.11.html>
- [11] <http://www.etsi.org/frameset/home.htm?/technicalactiv/Hiperlan/hiperlan2.htm>
- [12] http://www.dvb.org/dvb_technology/whitepaper-pdf-docs/dvbtpaper.pdf
- [13] K. Thomas and H. Lajos, "Adaptive Multicarrier Modulation: A Convenient Framework for Time-Frequency Processing in Wireless Communications" IEEE processing of the IEEE, vol. 88, No.5, pp.611-640, May 2000
- [14] Chi-Tsong Chen "System and Signal Analysis" Thomson, 1988
- [15] Poularikas, Alexander D. "The handbook of formulas and tables for signal processing", Springer, 1999

- [16] T. S. Rappaport, "Wireless Communications: Principles & Practice", Prentice Hall, 1995
- [17] Ochiai, H. and Imai, H.; "MDPSK-OFDM with highly power-efficient block codes for frequency-selective fading channels" Vehicular Technology, IEEE Transactions on, vol. 49 Issue: 1, pp. 74 –82, Jan. 2000
- [18] Cimini, L.J., Jr. and Sollenberger, N.R.; "Peak-to-average power ratio reduction of an OFDM signal using partial transmit sequences", IEEE Communications Letters, vol. 4, Issue: 3, pp. 86 –88. Mar. 2000
- [19] Breiling, H.; Muller-Weinfurtner, S.H.; Huber, J.B.; "SLM peak-power reduction without explicit side information", IEEE Communications Letters, vol. 5 Issue: 6, pp. 239 –241, Jun.2001
- [20] Ochiai, H. and Imai, H.; "Performance of the deliberate clipping with adaptive symbol selection for strictly band-limited OFDM systems ", Selected Areas in Communications, IEEE Journal on, vol. 18, Issue: 11, pp. 2270 –2277, Nov 2000
- [21] Nikookar, H. and Lidsheim, K.S.; "Random phase updating algorithm for OFDM transmission with low PAPR", Broadcasting, IEEE Transactions on, vol. 48 Issue: 2, pp. 123 –128, Jun. 2002.
- [22] Heung-Gyoon Ryu and Kyoung-Jae Youn; "A new PAPR reduction scheme: SPW (subblock phase weighting)" Consumer Electronics, IEEE Transactions on, vol. 48 Issue: 1, pp. 81 – 89, Feb 2002
- [23] Bernard Skler, "Rayleigh Fading Channels in Mobile Digital Communication systems, part I: Characterization" <http://engr.smu.edu/~ebird/FadingArticle1.pdf>
- [24] W.C. Jakes, "Microwave Mobile Communication", Wiley, 1974
- [25] J. Armstrong, "Analysis of new and existing methods of reducing intercarrier interference due to carrier frequency offset in OFDM", IEEE Transactions on Communications, vol. 47, pp. 365-369, March 1999.
- [26] Schafhuber, D.; Matz, G.; Hlawatsch, F.; "Pulse-shaping OFDM/BFDM systems for time- varying channels: ISI/ICI analysis, optimal pulse design, and efficient implementation", Personal, Indoor and Mobile Radio Communications, 2002. The 13th IEEE International Symposium on, vol. 3, 2002, pp. 1012 –1016
- [27] Andreas F. Molisch, "Wideband Wireless Digital Communications" Prentice, 2001
- [28] John G. Proakis, "Digital Communications" McGraw-Hill, 2000
- [29] Russell, M.; Stuber, G.L.; "Interchannel interference analysis of OFDM in a mobile

environment”, Vehicular Technology Conference, 1995 IEEE 45th, vol. 2, pp. 820 –824, Jul. 1995

[30] Ye Li; Cimini, L.J., Jr.; “Bounds on the Interchannel interference of OFDM in time-varying impairments” Communications, IEEE Transactions on, vol. 49 Issue: 3, pp. 401 – 404, Mar. 2001

[31] <http://www.raltron.com/products/clocks/default.asp>

[32] Yuping Zhao; Haggman, S.-G.; “Intercarrier interference self- cancellation scheme for OFDM mobile communication systems” Communications, IEEE Transactions on, Volume: 49 Issue: 7, pp. 1185 –1191, Jul. 2001

[33] Liu, H. and Tureli, U.; “A high-efficiency carrier estimator for OFDM communications ”, IEEE Communications Letters, vol. 2 Issue: 4, pp. 104 –106, Apr. 1998

[34] Ghogho and M.; Swami, A.; “Blind frequency-offset estimator for OFDM systems transmitting constant-modulus symbols”, IEEE Communications Letters, Volume: 6 Issue: 8, pp. 343 –345, Aug. 2002

[35] Sun-Yuan Kung; Yunnan Wu; Xinying Zhang; “Bezout space-time precoders and equalizers for MIMO channels”, Signal Processing, IEEE Transactions on, vol. 50, Issue: 10, pp. 2499 –2514, Oct. 2002

[36] Biao Chen and Hao Wang; “Maximum likelihood estimation of OFDM carrier frequency offset” ICC 2002 IEEE International Conference on, vol. 1, 2002 pp. 49 -53;

[37] Jian Li; Guoqing Liu; Giannakis, G.B.; “Carrier frequency offset estimation for OFDM-based WLANs”, IEEE Signal Processing Letters, vol. 8 Issue: 3, pp. 80 –82, Mar. 2001

[38] Muller-Weinfurtner, S.H.; “Optimum Nyquist windowing in OFDM receivers” Communications, IEEE Transactions on, vol. 49 Issue: 3, pp. 417 –420, Mar. 2001

[39] Li, Y.G.; Winters, J.H.; Sollenberger, N.R.; “MIMO-OFDM for wireless communications: signal detection with enhanced channel estimation” Communications, IEEE Transactions on, vol. 50 Issue: 9, pp. 1471 –1477, Sep. 2002

[40] Stamoulis, A.; Diggavi, S.N.; Al-Dhahir, N.; “Interchannel interference in MIMO OFDM”, Signal Processing, IEEE Transactions on, vol. 50 Issue: 10, pp. 2451 –2464, Oct. 2002

[41] Sun-Yuan Kung; Yunnan Wu; Xinying Zhang; “Bezout space-time precoders and equalizers for MIMO channels”, Signal Processing, IEEE Transactions on, vol. 50

Issue: 10, pp. 2499 –2514, Oct. 2002

[42] Tureli, U.; Liu, H.; Zoltowski, M.D.; “OFDM blind carrier offset estimation: ESPRIT ”, Communications, IEEE Transactions on, vol. 48 Issue: 9, pp. 1459 –1461, Sep. 2000

[43] Ming-Xian Chang; Su, Y.T.; “Blind joint channel and data estimation for OFDM signals in Rayleigh fading”; Vehicular Technology Conference, 2001. VTC 2001 Spring. IEEE VTS 53rd, vol.2, 2001; pp. 791 -795

[44] Redfern, A.J.; “Receiver window design for multicarrier communication systems ”, Selected Areas in Communications, IEEE Journal on, vol. 20 Issue: 5, pp. 1029 –1036, Jun. 2002

Vita

Yao Xiao was born in China in November, 1974. He studied control and systems at Dalian University of Technology and achieved the degree of Bachelor of Science in electrical engineering in July 1998. He then furthered his study in the Institute of Automation, Chinese Academic of Sciences, and graduated with a master degree of control theories and applications in July 2001. Then he entered the master's program in the Department of Electrical and Computer Engineering at Louisiana State University in the fall of 2001. Now he is a candidate for the degree of Master of Science in Electrical Engineering. In the meantime, he is studying toward a doctorate degree in electrical engineering at Louisiana State University.